J. Rubb. Res., **15(2)**, 111–123

FEA Modelling of Stress Distributions in Concrete Test Specimens Compressed through Rubber Sheets

ISMALIZA ISMAIL*# AND JULIA GOUGH**

A Finite Element (FE) study of the behaviour of concrete blocks compressed against rubber sheets was conducted. The results were compared to experimental tests of the same assembly reported in literature. It was found that tensile stresses developed within the concrete due to non-uniform compression of the rubber and were likely to have been the cause of failure of the concrete except where the rubber sheet was very thin or absent. The effect disappeared if contact between the rubber and concrete was frictionless.

Keywords: concrete; rubber; stress; compression; FEA

Unbonded rubber pads are sometimes used to provide compliance between concrete or steel elements of engineering structures. Compliant elements might be needed to reduce transmission of vibration, to allow for thermal expansion and subsidence movements, or to reduce local stresses arising from misalignment of the surfaces. An example of a floating slab light-rail track, in which the rail track is mounted on rubber bearings to reduce ground borne noise and vibration is shown in *Figure 1*.

A theoretical investigation of the stresses in concrete blocks loaded through rubber pads was carried out by Coveney *et al.*[1] Recent work[2] has uncovered an error in this treatment but also showed that the stress state in the concrete strongly depended on the boundary conditions. In other words, it depended on the relative dimensions of the rubber and concrete and how they were supported.

Newman and Lachance[3] made an experimental study of the effects of different packing materials interposed between steel platens and cylindrical or cuboidal concrete test specimens on the lateral deformation and failure load. They found that the crushing strength of concrete cubes decreased with increasing thickness of an interposed rubber sheet and the mode of failure changed from an apparent compression failure to a vertical splitting failure. They suggested that as the rubber tended to squeeze out at the sides, the vertical load was concentrated towards the centre of the concrete specimen and that soft materials introduced a complex stress distribution near the ends of the concrete specimen, radically altering its failure mode.

*Rubber Research Institute of Malaysia, Malaysian Rubber Board, P.O. Box 10150, 50908, Kuala Lumpur, Malaysia
**Tun Abdul Razak Research Centre, Brickendonbury, Hertford, SG13 8NL, United Kingdom
Corresponding author (e-mail: ismaliza@lgm.gov.my)

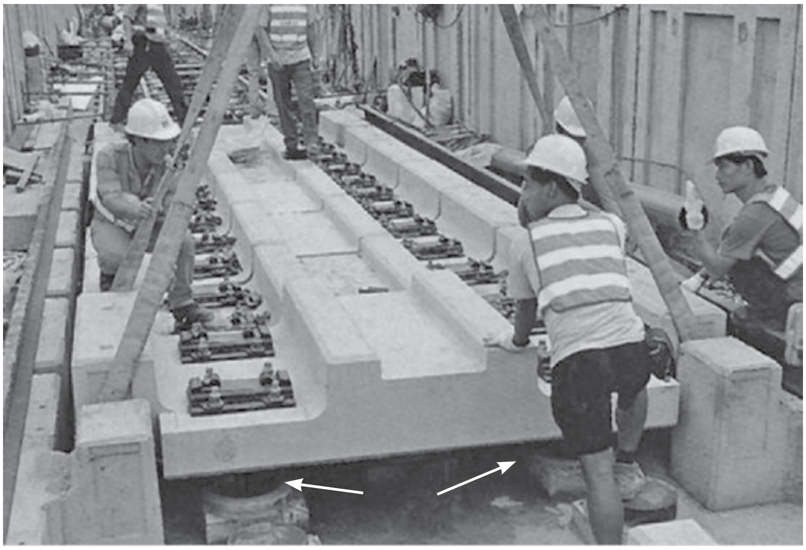

Figure 1. Installation of floating slab track for Hong Kong Airport rail link. Arrows show location of rubber bearings. (From www.urbantransport-technology.com/projects/hong_kong)

Griffith[4] postulated that the failure in brittle solids is caused by the growth of a small flaw, which might reasonably be expected to exist in porous materials such as concrete. The fracture mechanics calculations, based on Griffith's hypothesis may be used to relate the applied stresses to the energy released as the flaw grows. It is assumed that there are many randomly oriented flaws so that one of them will be oriented in the most damaging direction. In this way Sack[5] has shown, by considering a tensile stress acting perpendicular to the plane of a penny-shaped crack in an elastic medium, that the tensile strength of brittle materials is not affected by the stresses acting in the plane of the crack. A similar suggestion has been attributed to Rankine and is known as the maximum principal stress or Rankine failure criterion[6]. Fracture mechanics is also helpful in explaining why the strength of concrete in uniaxial tension is much smaller than in uniaxial compression; crack opening under tensile stress is a more effective means of releasing energy than crack shearing which might occur under a system of unequal triaxial compressive stresses.

The strength of concrete in uniaxial tension is typically only of the order of one tenth of its value in compression[7] and thus concrete is virtually never put in tension; careful design and the use of rebars and tendons ensure that only compressive stresses develop under load. In this case, Sack's equation is no longer useful and recourse is made to various empirical failure criteria, such as the Mohr-Coulomb[8] failure criteria, to describe a failure envelope for triaxial compressive stress systems.

The purpose of this work is to simulate the Newman and Lachance experiment in order to understand the stress and strain profiles and failure mechanisms of concrete blocks compressed through rubber sheets. Attention was focused on the maximum principal stress because, according to Sack's or Rankine's hypothesis, it is this stress, if tensile, that is likely to lead to failure of the concrete.

ANALYSIS METHOD

Abaqus/Standard version 6.9 was used for the analysis. A schematic diagram of the FE model is shown in *Figure 2*. It consisted of a concrete block, 102 mm wide, compressed by a steel platen with a rubber sheet interposed between them. The heights of the concrete blocks and thickness of the rubber sheets were varied and corresponded to those used by Newman and Lachance[3]. Although Newman and Lachance tested blocks of square cross-section, two dimensional plane strain analyses were carried out to reduce the need for complex meshing and minimise the run times of the models. It was expected that 2D and 3D analyses would give qualitatively similar results. The rubber material was represented by a neo-Hookean strain energy function[9] with a shear modulus of 1 MPa and bulk modulus of 2000 MPa using hybrid linear reduced integration elements (type CPE4RH). The concrete was modelled as a linear elastic material with Young's modulus of 36.3 GPa and Poisson's ratio of 0.15, in accordance with the properties reported by Newman and Lachance, with linear, reduced integration CPE4R elements. The steel was modelled as a linear elastic material with Young's Modulus of 210 GPa and Poisson's ratio of 0.3 with CPE4R elements. For simplicity, one quarter of the compression test system was modelled and appropriate symmetry boundary conditions were applied to represent the rest of the system. The mesh density was much finer near the contact region where the stress gradients were expected to be highest. The compression was applied at the bottom of the steel platen as shown in *Figure 2* as a fixed displacement.

The coefficient of friction for rubber falls with increasing normal load so that for high loads the frictional force is constant[10], and depends on sliding speed, as well as on the roughness of the contact surfaces. However, since no direct experimental measurement of the friction coefficient was made for the Newman and Lachance experiment, a simple friction model with constant coefficient of friction was assumed. Friction coefficients of 0.6 and 0.45 between the rubber and concrete were modelled with a Coulomb friction model with the default penalty friction formulation available in Abaqus/Standard. These values were thought to be reasonable for normal stresses of the order of 10 MPa[11], as used in Newman and Lachance's experiments. A no-slip condition, imposed with a tying constraint, and frictionless interfaces were also modelled. The friction coefficient between the rubber and steel was always assumed to be the same as that between the rubber and concrete. It would be straightforward to introduce a pressure dependency of the coefficient of friction into the model if suitable data were available.

RESULTS AND DISCUSSION

Effect of Rubber Thickness

The behaviour of a 102 mm thick concrete plane strain block, loaded through rubber sheets of various thicknesses was simulated. A coefficient of friction of 0.6 between the rubber and concrete and between the rubber and steel was assumed. The compressive load was the same per unit area as the failure load reported by Newman and Lachance in compression experiments on 102 mm concrete cubes. The cubes, after failure, are shown in *Figure 3* and the failure loads are given in *Table 1*.

For the geometry under consideration the maximum principal stress was found to be almost coincident with the lateral stress, S_{11}, where the 1-direction is parallel to the contact surface. The lateral stress distributions are shown in *Figure 4*. The position of the crack observed by Newman and Lachance is superimposed on *Figure 4* for comparison.

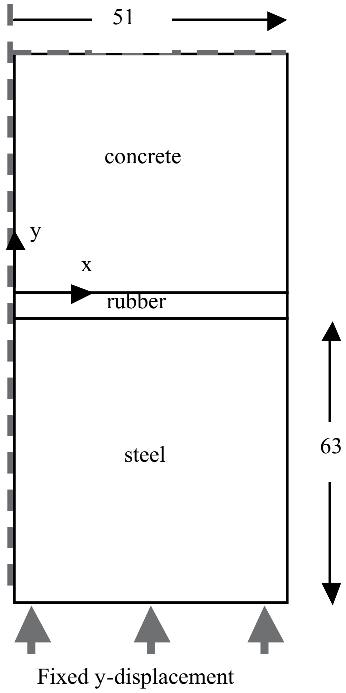

Figure 2. Schematic diagram of plane strain FEA model for compression of concrete block with rubber sheet. Dashed lines represent symmetry planes. Dimensions in mm.

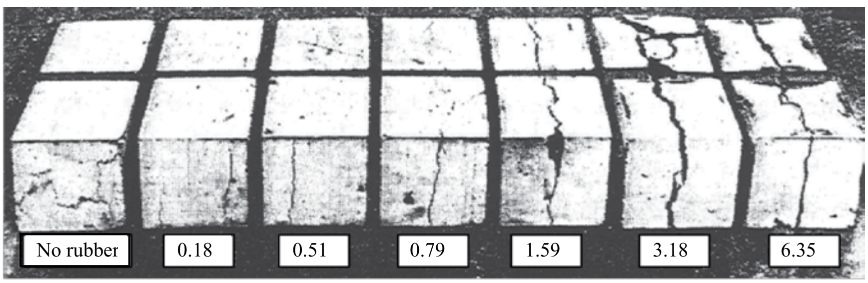

Figure 3. Variation of mode of failure in 102 mm concrete cubes with thickness of rubber sheet, shown in mm. From Newman and Lachance[3].

TABLE 1. MAXIMUM PRINCIPAL STRESS IN 102 mm CONCRETE PLANE STRAIN BLOCKS OR CUBES

Rubber thickness (mm)	Experimental failure load Newman and Lachance[3] (kN)	Maximum tensile principal stress (FEA) (MPa)
6.35	99	2.02
3.18	128	2.60
0.79	194	1.35
0.18	257	0.91
0	353	0.03

The vertical stress distributions, S_{22} are shown in *Figure 5*. The maximum principal tensile stress is reported in *Table 1*.

The mean lateral strain, $\bar{\varepsilon}_x$, was calculated as

$$\bar{\varepsilon}_x = \frac{u_x}{D} \qquad \dots 1$$

where D is the half-width of the block and u_x is the maximum lateral displacement (i.e. of points initially at $x = D$). It is plotted in *Figure 6* for plane strain blocks compressed to a load of 455 N/mm over the half-width, corresponding to a load of 93 kN on 102 mm cubes.

The position of the main crack in the Newman and Lachance experiments coincides with the location of the maximum lateral stress in the simulations and moves from the centre of the concrete for compression through thick rubber sheets to the side when the rubber is thin. The failure load reported by Newman and Lachance decreased markedly as the rubber sheet thickness was increased. For the three thickest rubber sheets investigated, the maximum principal stress under the failure load is about 2 MPa. This is in satisfactory agreement with literature values for the tensile strength of concrete[7] and suggests that these blocks failed in tension. The reduction in load at failure can be explained by noting the comparatively large compression of the thicker rubber under relatively modest loads and that the thickness of the deformed sheet is very non-uniform – being thicker in the centre than at the sides. The tensile stress in the concrete appears to arise from this non-uniform compression, rather than from lateral spread of the rubber inducing tensile stresses at the rubber concrete interface as was suggested previously[1,3]. In fact, the lateral stress at the rubber concrete interface is compressive; the maximum tensile stress occurs at the mid-height of the concrete block.

As the rubber thickness is reduced, the rubber deformation for a given strain reduces and the rubber stiffness increases relative to the concrete. The compression stiffness per unit depth of a plane strain rubber sheet of thickness, t, bonded between two rigid surfaces, is given to a good approximation by[12]:

$$k_r = \frac{8GKD\,(1 + S^2)}{t[4G(1 + S^2) + K]} \qquad \dots 2$$

where G is the shear modulus and K is the bulk modulus of the rubber and S is the shape factor of the block, given by D/t. The stiffness per unit depth of the concrete is given by

$$k_c = \frac{2ED}{T} \qquad \dots 3$$

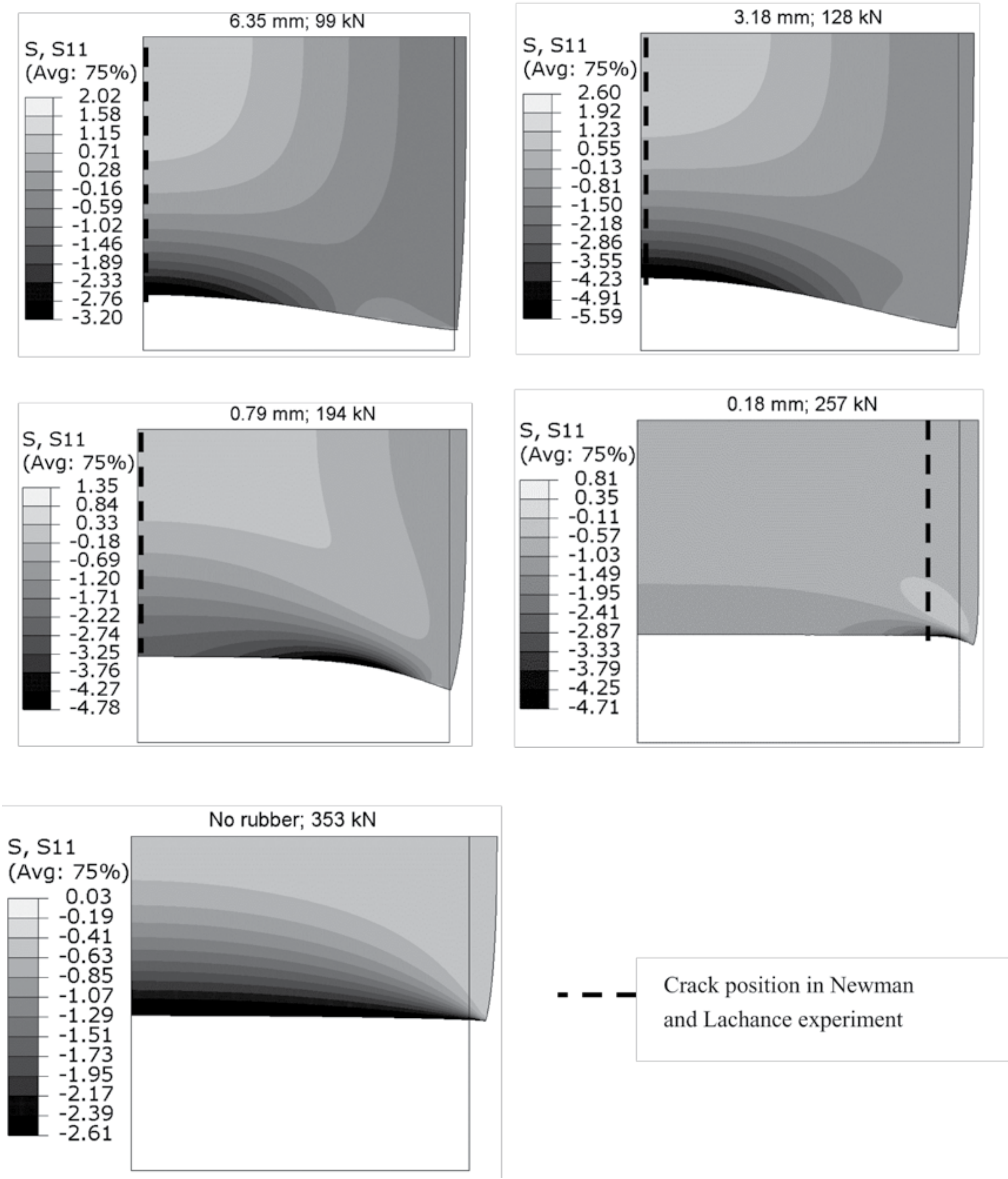

Figure 4. Lateral stress distributions in a concrete plane strain block loaded through rubber sheets under compressive loads corresponding to failure loads in experiments of Newman and Lachance[3]. The rubber sheet thicknesses and compressive load are shown above each plot. Concrete deformations are scaled by a factor of 500. For clarity, the rubber and steel are not shown on the plots.

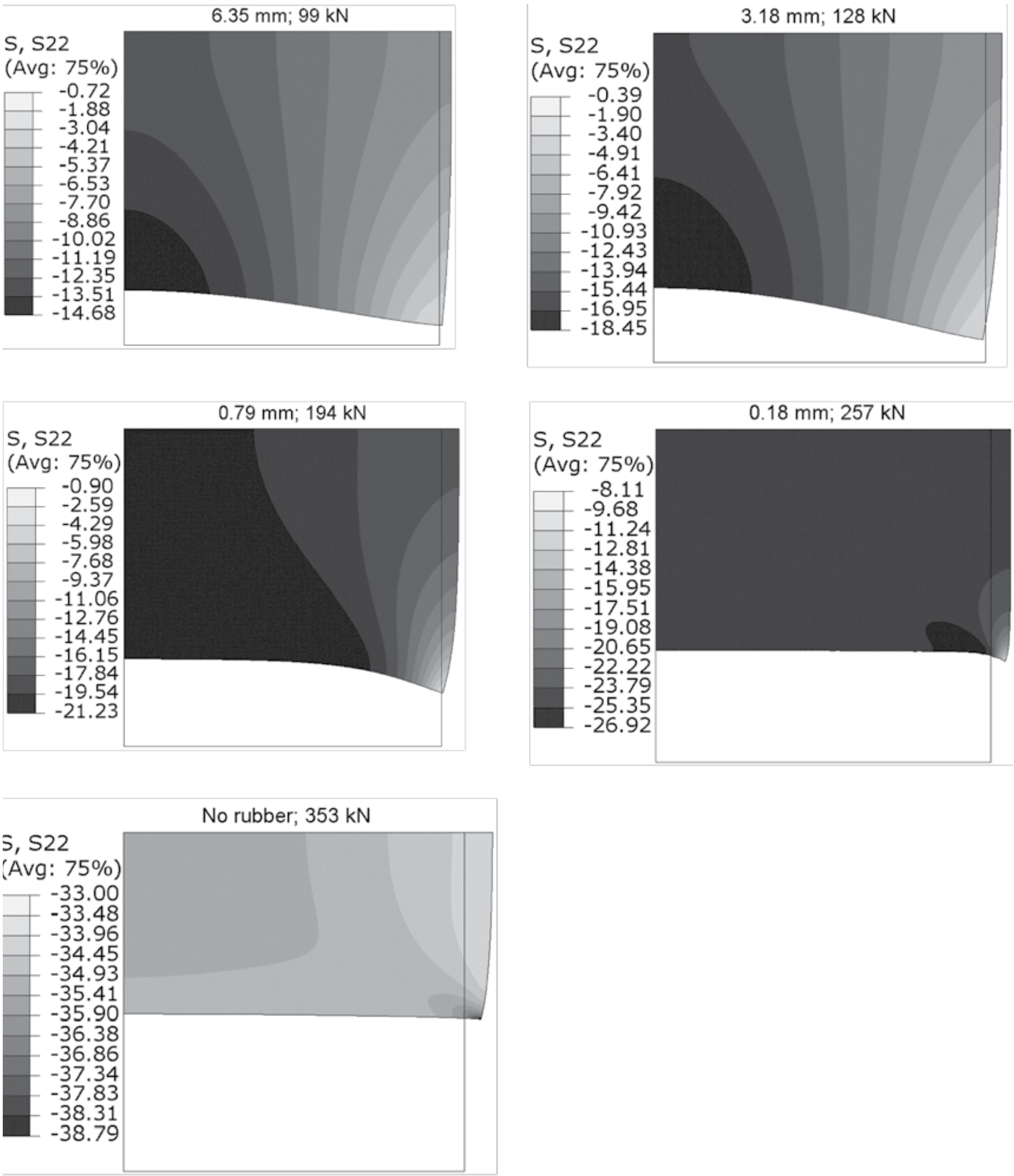

Figure 5. Vertical stress distributions in a concrete plane strain block loaded through rubber sheets under compressive loads corresponding to failure loads in experiments of Newman and Lachance[3]. The rubber sheet thicknesses and compressive load are shown above each plot. Concrete deformations are scaled by a factor of 500. For clarity, the rubber and steel are not shown on the plots.

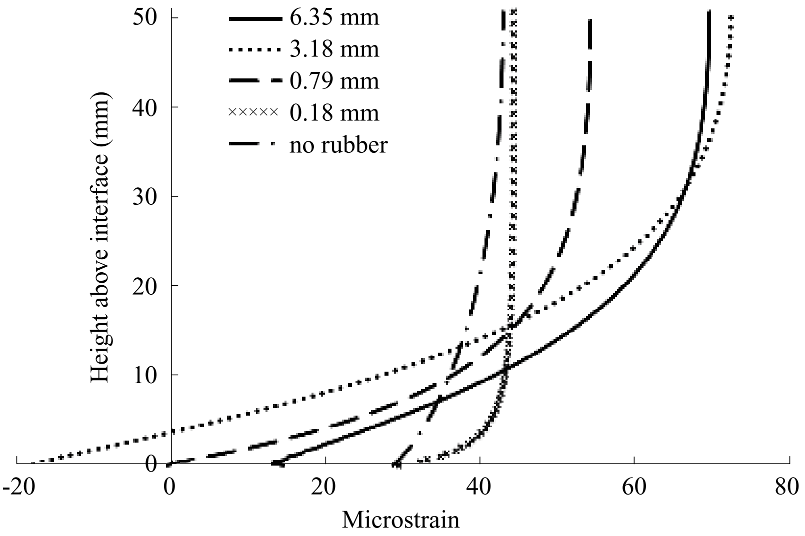

Figure 6. Lateral strain profiles of 102 mm thick concrete plane strain blocks compressed through rubber sheets of different thicknesses under a compressive load corresponding to 93 kN on 102 mm cubes.

where E is Young's modulus of the concrete and T is its thickness. This gives stiffnesses of the 6.35 mm and 3.18 mm thick rubber sheets of about 10% and 60% respectively of that of the concrete. *Equation 2* breaks down when the rubber stiffness is of the same order of that of the concrete because the assumption of rigidity of the bounding surfaces is no longer valid, but it is clear that for thin sheets, if there is no lateral slip, the rubber is stiffer than the concrete. Consequently, the differential compression of the rubber across its width becomes negligible and the tensile stress in the concrete diminishes. A different failure mechanism, such as splitting along planes at 45° to the loading direction, is likely to have occurred in the block where no rubber sheet was present because even under very large compressive loads the tensile stress was negligible. This is supported by the absence of a central vertical crack in this block.

Figure 6 shows that the mean lateral strain in the concrete under a fixed load was greatest for loading through thick rubber sheets and occurred at the mid-height of the concrete. This also supports the suggestion that these blocks failed in tension at their mid-height.

Effect of Concrete Thickness

A friction coefficient of 0.6 between the rubber and concrete and between the rubber and steel was used and a compressive load of 455 N/mm over the half-width, corresponding to a load of 93 kN on 102 mm cubes, was applied. Plots of the lateral stress for various heights of concrete loaded through a 6.35 mm rubber sheet are shown in *Figure 7*. The lateral strain profiles for a 305 mm high concrete plane strain block compressed between various thicknesses of rubber are shown in *Figure 8*. The lateral strain measurements of Newman and Lachance for a 305 mm high square block compressed to 93 kN through a 3.18 mm rubber sheet are also shown in *Figure 8* for comparison. The lateral strain

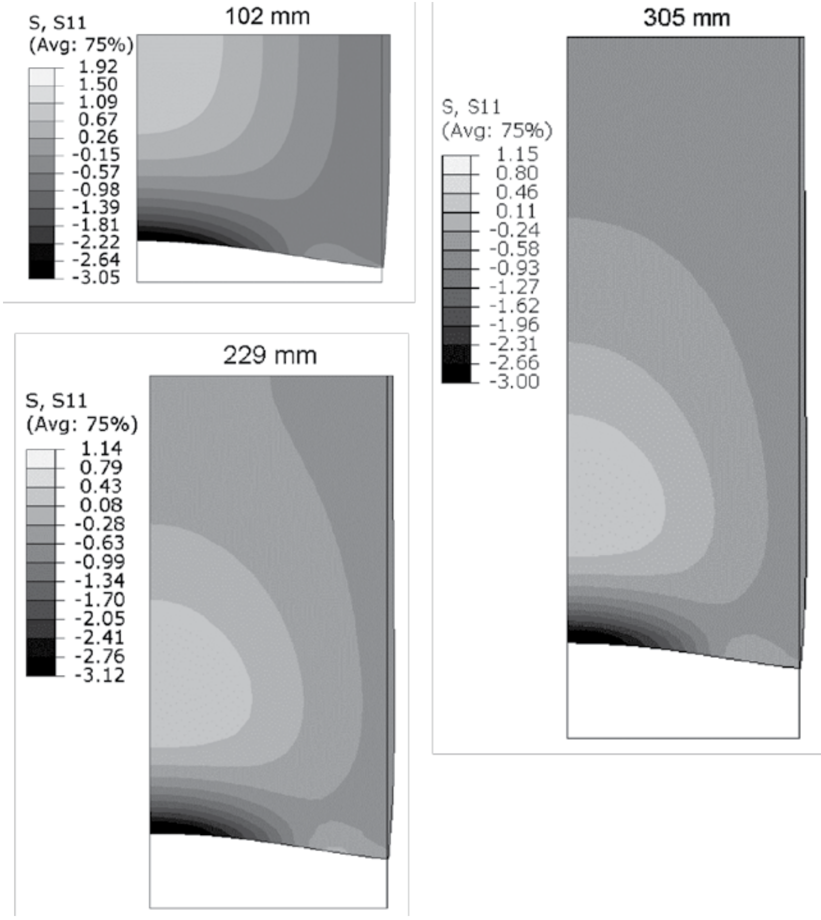

Figure 7. Lateral stress distributions in concrete plane strain blocks of various heights, as shown above the plots, loaded through 6.35 mm thick rubber sheets to a load corresponding to 93 kN on 102 mm cubes. Concrete deformations are scaled by a factor of 500.

profiles for different heights of concrete are shown in *Figure 9*.

For concrete blocks taller than their width, the maximum tensile strain no longer occurs at the mid-height of the block, but at a height approximately equal to half of the width. The profile of the deformed plane strain block compressed through a 3.18 mm rubber sheet agrees well with the measurements of Newman and Lachance although the strains were somewhat larger in the simulations. This is due at least in part to the use of a plane strain model; because no strain is permitted perpendicular to the measurement we would expect the lateral strains to be larger than for a block of cubic cross-section as used by Newman and Lachance. A three-dimensional simulation was carried out and gave adequate agreement with the measurements, though the strain now varied through the depth of the concrete.

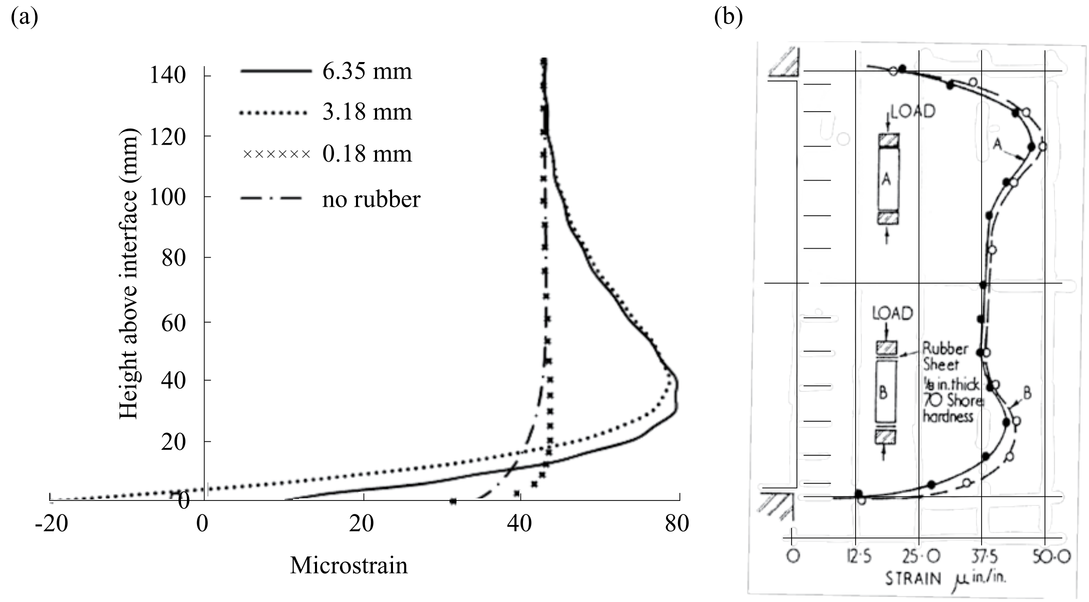

Figure 8. (a) Lateral strain profiles for 305 mm high concrete plane strain block compressed through various thicknesses of rubber sheet to a load corresponding to 93 kN on 102 mm cubes. (b) (Dashed line): measured profile of 305 mm high concrete prism compressed to 93 kN through 3.18 mm thick rubber sheets[3].

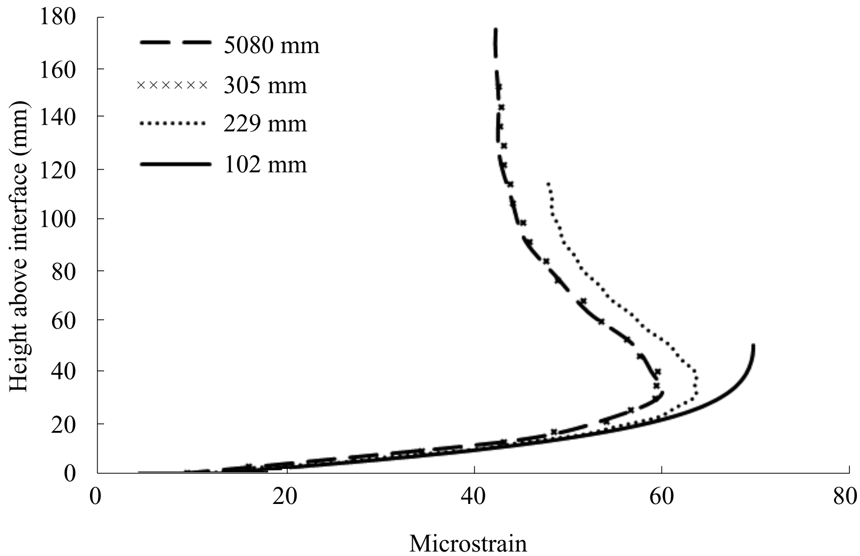

Figure 9. Lateral strain profiles for concrete plane strain blocks of various heights compressed through 6.35 mm thick rubber sheets to a load corresponding to 93 kN on 102 mm cubes.

Effect of Friction

A 102 mm thick concrete plane strain block compressed under a 6.35 mm rubber sheets, with various levels of friction at the rubber concrete interface, was simulated. When the interface was frictionless the model only converged for a small applied load. This was attributed to high distortion of the elements at the edge of the contact region as the rubber squeezed out. In order to aid comparison between the results under different normal loads, the stresses were normalised by dividing by the average normal pressure over the contact region. The maximum tensile stress was found to occur in the centre of the block for friction coefficients of 0.45, 0.6 and infinity (tied). In the case of frictionless contact, the normalised lateral stress was very small everywhere.

The variation of normalised lateral stress with position across the width of the block at its centre-height is shown in *Figure 10*. The lateral position from the centre of the block has been normalised by dividing by the half-width, D. The tensile stress reaches a maximum at an intermediate level of friction, corresponding to the greatest thickness variation of the deformed rubber sheet. As the friction level is reduced from a fully bonded interface, slip occurs at the edges of the sheet and, due to the near incompressibility of rubber, the rubber becomes thinner as it squeezes out laterally. The region of slip increases as the friction coefficient is reduced so that with a near-frictionless condition slip occurs across the full width. The strain distribution in the rubber is then uniform and there is no differential thinning across the width of the sheet. Hence, the differential compression of the concrete, and consequently the maximum principal stress, decreases.

Coveney *et al.*[1] derived an expression for the position of the slip / no slip boundary for a

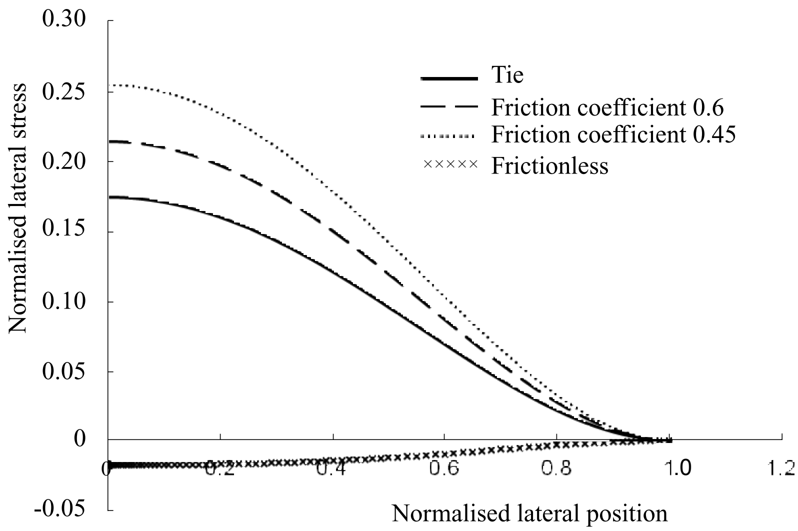

Figure 10. Effect of friction on normalised lateral stress at the centre-height of a plane strain concrete block compressed by 6.35 mm thick rubber sheet.

TABLE 2. POSITION OF SLIP / NO-SLIP BOUNDARY FOR A RUBBER-CONCRETE INTERFACE OF HALF-WIDTH 51 mm AND COEFFICIENT OF FRICTION OF 0.6 UNDER A SMALL COMPRESSION

Rubber thickness (mm)	Position from centre of slip / no-slip boundary (*Equation 4*) (mm)	Position from centre of slip / no-slip boundary (FEA) (mm)
6.35	36.7	38.1
3.18	41.6	41.9
0.79	47.5	47.6
0.18	49.8	49.5

plane stain elastic sheet squeezed between two rigid surfaces. Their expression is

$$\frac{3d}{2t} = \mu \exp\left[\frac{2\mu}{t}(D-d)\right] \qquad \ldots 4$$

where, μ is the coefficient of friction and d is the distance from the centre of the interface to the slip / no slip boundary. The theoretical values calculated from *Equation 4* are compared in *Table 2* with those obtained from the FEA for a small applied load. There was good agreement, although the theory cannot predict the subsequent stick-slip behaviour as the load is increased.

CONCLUSIONS

When concrete is loaded through rubber sheets a complex non-uniform stress distribution is produced near the ends of the concrete. Unless the rubber sheet is very thin, the coefficient of friction is very low, or the concrete block is extremely large[2] non-uniform compression of the rubber sheet causes tensile stresses to develop in the concrete. The maximum tensile stress occurs at a distance of around half the concrete width into the concrete. Under sufficient compressive load, these tensile stresses are likely to cause tensile fracture of the concrete. Intermediate levels of friction give rise to the highest tensile stresses.

ACKNOWLEDGEMENT

The authors wish to thank Dr. A.H. Muhr for suggesting this area of work, helpful discussions and for commenting on the manuscript.

Date of receipt: July 2011
Date of acceptance: November 2011

REFERENCES

1. COVENEY, V.A., FULLER, K.N.G. AND MUHR, A.H. (1990) Stresses Developed in Rubber/Concrete Contacts in Contact in Stress Analysis. (*Roberts A.D. and Mottershead J.E. eds*) London: Institute of Physics. pp. 63–78.

2. GOUGH, J. AND MUHR, A.H. (2012) Stresses in Concrete Blocks Loaded through Rubber Pads. In preparation.

3. NEWMAN, K. AND LACHANCE, L. (1964) The Testing of Brittle Materials under Uniform Uniaxial Compressive Stress. Proc. ASTM, **64**, 1044-1067.

4. GRIFFITH, A.A. (1920) The Phenomenon of Rupture and Flow in Solids. *Philos. Trans. R. Soc.*, **A221**, 163–198.

5. SACK, R.A. (1946) Extension of Griffith's Theory of Rupture to Three Dimensions. *Proc. Phys. Soc.*, **58**, 729–736.

6. TIMOSHENKO, S. (1956) Strength of Materials, Part II, Advanced Theory and Problems. 3rd Edn. Princetown: Van Nostrand.

7. NEVILLE, A.M. (1973) Properties of Concrete. London: Pitman.

8. COULOMB, C.A. (1776) Essai sur une Application des Règles des Maximis et Minimis à quelquels Problèmes de Statique Relatifs, à l'architecture. *Mémoires de Mathématique et de Physique*, **7**, 343–382.

9. RIVLIN, R.S. (1948) Large Elastic Deformations of Isotropic Materials, I Fundamental Concepts. *Philos. Trans. R. Soc.*, **A240**, 459–490.

10. SCHALLAMACH, A. (1958) Friction and Abrasion of Rubber. *Wear*, **1**, 384–417.

11. GOUGH, J., MUHR, A.H. AND KWONG, M. (2001) Measurement and Modelling of Friction of Rubber. *Constitutive Models for Rubber II*. (*Besdo D., Schuster R.H. and Ihlemann J. eds*.) Netherlands: Balkema, 165–171.

12. GENT, A.N. AND LINDLEY, P.B. (1959) The Compression of Bonded Rubber Blocks. *Proc. Instn. Mech. Engrs*., **173**, 111–122.